Miscibility studies of poly(vinyl chloride) with polyacrylates: The thermodynamic and phase behaviour

C. K. Sham* and D. J. Walsh†
Department of Chemical Engineering and Chemical Technology, Imperial College, London SW7 2BY, UK
(Received 13 May 1986; revised 11 July 1986)

The miscibilities of poly(vinyl chloride) (PVC) with poly(n-propyl acrylate), poly(n-butyl acrylate) and poly(n-pentyl acrylate) were studied. They were found to be miscible over the whole composition range at room temperature. Light-scattering turbidity, electron microscopy and glass-transition-temperature measurements showed them to phase-separate at higher temperatures. The phase diagrams of the various mixtures were determined. The polyacrylates with a higher concentration of carbonyl functional groups showed a higher phase-separation temperature. When the Flory equation-of-state theory was applied to the systems, a negative interaction entropy parameter Q_{12} had to be introduced to counterbalance the large negative interaction energy parameter X_{12}, obtained from the heats of mixing of the oligomeric analogues, which resulted in the simulated spinodals being flat-bottomed. However, if a much smaller negative X_{12} was used, with a smaller Q_{12}, the calculated spinodal had more curvature and corresponded closely to the measured phase-separation points.

(Keywords: miscibility; poly(vinyl chloride); thermodynamics; phase behaviour)

INTRODUCTION

Poly(vinyl chloride) (PVC) has been found to be miscible with a wide range of polymers containing electron donor groups such as esters. This has been attributed to the formation of specific interactions involving the methine hydrogen of PVC[1,2], which give favourable heats of mixing. In previous papers[3-7], we have established the miscibility of PVC with various polyacrylates and polymethacrylates. The blends of PVC with poly(n-propyl acrylate) (PPrA) and poly(n-butyl acrylate) (PBA) were found to phase-separate on heating, but the results on poly(n-pentyl acrylate) (PPeA) blends were rather ambiguous. The heats of mixing of oligomeric analogues of various polyacrylates and polymethacrylates with a chlorinated paraffin (as an analogue for PVC) have been found to be consistent in most cases with the miscibility of the respective polymers[8].

In principle, thermodynamic theories can predict or describe phase-separation behaviour. A theoretical phase diagram consists of binodal curve and spinodal curve. The binodal curve is the line joining the compositions of phase-separated mixtures at equilibrium, which is given by

$$(\Delta\mu_1)_A = (\Delta\mu_1)_B \qquad (\Delta\mu_2)_A = (\Delta\mu_2)_B \qquad (1)$$

where $(\Delta\mu_i)_A$ and $(\Delta\mu_i)_B$ are the chemical potentials of mixing of component i at two compositions A and B, on the binodal at a given temperature. The spinodal curve lies inside the binodal and it represents the limit of metastable compositions given by

$$\partial^2(\Delta G)/\partial\phi^2 = 0 \qquad (2)$$

where ϕ is the segment fraction of either component. The binodal and spinodal meet at the critical point, where

$$\partial^3(\Delta G)/\partial\phi^3 = \partial^2(\Delta G)/\partial\phi^2 = 0 \qquad (3)$$

For a hypothetical polymer–polymer mixture, the contribution of the pure and the binary state parameters to the miscibility was examined by McMaster[9] using a modified version of the equation-of-state theory developed by Flory and coworkers[10-13]. He showed that the equation-of-state theory can predict both lower and upper critical solution temperature behaviour individually or simultaneously. Olabisi[14] and ten Brinke *et al.*[15] have also attempted to simulate the phase diagrams of polymer mixtures using the equation-of-state theory.

Using a modified version of the above theory, we have simulated the spinodal curves for various systems[16-19]. The procedure, in each case, was to calculate the interaction parameter X_{12} from heat-of-mixing measurements of low-molecular-weight analogues. The non-combinatorial entropy parameter Q_{12} was used to fit the minimum of the spinodal to the minimum of the cloud-point curve. Finally, the full spinodal curve was calculated using these values and compared with the

* Present address: Polymer Science and Engineering Department, University of Massachusetts, Amherst, MA, 01003, USA.
† To whom all correspondence should be addressed at his present address: Central Research and Development Department, E. I. Du Pont de Nemours and Co., Experimental Station, Wilmington, DE 19898, USA.

0032-3861/87/050804-09$03.00

measured cloud-point curve. The final calculated curves in many cases were flat-bottomed, suggesting that the X_{12} value used was too large. This could have been explained either by problems in the use of low-molecular-weight analogues in calculating X_{12} or by the known temperature dependence of X_{12} in some cases[20]. The temperature dependence of X_{12} is thought to arise from the dissociation of the specific interactions that are responsible for the miscibility of these polymers and has been demonstrated by infra-red spectroscopy measurements[21].

In this paper, we report the phase diagrams obtained for PVC with poly(n-propyl acrylate), poly(n-butyl acrylate) and poly(n-pentyl acrylate). We also describe the simulation of the spinodal curves using the above procedures.

THEORY

With the notation of Flory and coworkers, the heat of mixing of component 1 and component 2 is[11-13]

$$\Delta H_m = \bar{r}Nv^*\left[\phi_1 P_1^*\left(\frac{1}{\tilde{v}_1}-\frac{1}{\tilde{v}}\right)+\phi_2 P_2^*\left(\frac{1}{\tilde{v}_2}-\frac{1}{\tilde{v}}\right)+\frac{\phi_1\theta_2 X_{12}}{\tilde{v}}\right] \quad (4)$$

The chemical potential of component 1 in the mixture is given by

$$\frac{\Delta\mu_1}{RT}=\ln\phi_1+\left(1-\frac{r_1}{r_2}\right)\phi_2+\frac{P_1^*V_1^*}{RT}\left[3\tilde{T}_1\ln\left(\frac{\tilde{v}_1^{1/3}-1}{\tilde{v}^{1/3}-1}\right)+\frac{1}{\tilde{v}_1}-\frac{1}{\tilde{v}}+\tilde{P}_1(\tilde{v}-\tilde{v}_1)\right]+\frac{V_1^*\theta_2^2}{RT\tilde{v}}(X_{12}-TQ_{12}\tilde{v}) \quad (5)$$

Applying the spinodal condition, $\partial(\Delta\mu_1/RT)\partial\phi_2=0$, to equation (5) yields the equation used in the simulation of the spinodals[16-19]:

$$\frac{\partial}{\partial\phi_2}\left(\frac{\Delta\mu_1}{RT}\right)=-\frac{1}{\phi_1}+\left(1-\frac{r_1}{r_2}\right)+\frac{P_1^*V_1^*}{RT_1^*}\left(\frac{-D}{\tilde{v}-\tilde{v}^{2/3}}\right)+\frac{P_1^*V_1^*D}{RT\tilde{v}^2}+\frac{P_1V_1^*D}{RT}+\frac{V_1^*X_{12}2\theta_2^2\theta_1}{RT\tilde{v}\phi_1\phi_2}-\frac{V_1^*X_{12}D\theta_2^2}{RT\tilde{v}^2}-\frac{V_1^*Q_{12}2\theta_2^2\theta_1}{R\phi_1\phi_2} \quad (6)$$

where $D=\partial\tilde{v}/\partial\phi_2=-\partial\tilde{v}/\partial\phi_1$ given by (7)

$$\frac{\partial\tilde{v}}{\partial\phi_2}=\left[\frac{\partial\tilde{P}}{\partial\phi_2}-\frac{1}{\tilde{T}}\left(\tilde{P}+\frac{1}{\tilde{v}^2}\right)\frac{\partial\tilde{T}}{\partial\phi_2}\right]\Big/\left(\frac{2}{\tilde{v}^3}-\frac{\tilde{T}(\tilde{v}^{1/3}-\frac{2}{3})}{\tilde{v}^{5/3}(v^{1/3}-1)^2}\right) \quad (8)$$

$$\frac{\partial\tilde{P}}{\partial\phi_2}=\frac{P}{P^{*2}}\left[P_1^*-P_2^*-X_{12}\theta_2\left(1-\frac{\theta_1}{\phi_2}\right)\right] \quad (9)$$

and

$$\frac{\partial\tilde{T}}{\partial\phi_2}=\frac{T}{P^*}\left(\frac{P_2^*}{T_2^*}-\frac{P_1^*}{T_1^*}\right)+\frac{\tilde{T}}{P^*}\left[P_1^*-P_2^*+X_{12}\theta_2\left(1-\frac{\theta_1}{\phi_2}\right)\right] \quad (10)$$

In order to solve equation (6) to find the theoretical phase-separation temperature, we require the hard-core and reduced variables, which can be obtained from the following parameters: (a) the specific volume $v_{sp}=1/\rho$; (b) the thermal expansion coefficient $\alpha=(1/v)(\partial v/\partial T)_P$; and (c) the thermal pressure coefficient $\gamma=(\partial P/\partial T)_V$. We would also require the following binary parameters: (d) the surface per unit of core volume ratio $S_2/S_1=S$; and (e) the interaction parameter X_{12}.

Accounting for the temperature dependence of v_{sp}, α and γ at atmospheric pressure[11-13],

$$v_{sp}=v_{sp}^\circ e^{\alpha\Delta T} \quad (11)$$

$$\alpha=\alpha_0+\alpha_0^2(7+4\alpha_0T)\Delta T/3 \quad (12)$$

$$\gamma=\gamma_0-\gamma_0(1+2\alpha_0T)\Delta T/T \quad (13)$$

values of $\tilde{v}$, P^* and $\tilde{T}$ could be found for each component at zero pressure from

$$\tilde{v}_i^{1/3}=1+\alpha_iT(3+3\alpha_iT) \quad (14)$$

$$P_i^*=\gamma_iT\tilde{v}_i^2 \quad (15)$$

$$\tilde{T}_i=(\tilde{v}_i^{1/3}-1)/\tilde{v}_i^{4/3} \quad (16)$$

and for the mixture

$$P^*=P_1^*\phi_1+P_2^*\phi_2-\phi_1\theta_2X_{12} \quad (17)$$

where

$$\theta_2=S\phi_1/(S\phi_1+\phi_2) \quad (18)$$

$$T^*=P^*/[(\phi_1P_1^*/T_1^*)+(\phi_2P_2^*/T_2^*)] \quad (19)$$

$$\tilde{T}=T/T^* \quad (20)$$

and, by iteration, $\tilde{v}$ for the mixture can be found from the equation of state

$$\tilde{v}^{1/3}=1/(1-\tilde{T}\tilde{v}) \quad (21)$$

Alternatively, at a single temperature where both α and γ are known, P_i^* and $\tilde{T}_i$ can be calculated from equations (11), (12) and (13), and hence T_i^*. One can then calculate P^* and T^* for the mixture, and $\tilde{T}$ for either the mixture or both components can be found from equation (20) at any temperature, and hence $\tilde{v}$. The procedure would give the same result except when the ratio of the two components is very large or small, and the equations become very sensitive to small errors in $\tilde{v}$.

The interaction parameter X_{12} can be obtained by fitting equation (4) to the experimental heats of mixing of low-molecular-weight analogues.

EXPERIMENTAL

Preparation of monomers and polymers

The monomers, n-propyl acrylate and n-pentyl acrylate, were prepared by the acid-catalysed *trans*-esterification of methyl acrylate with the respective normal alcohols. The reaction was shifted to the desired direction by distilling off the low-boiling alcohol as soon

as it was formed. An inhibitor, hydroquinone, was used as a radical quencher to prevent the polymerization of acrylic acid ester during the reaction.

The alcohols, hydroquinone and *p*-toluenesulphonic acid (catalyst) used were AR grade supplied by BDH Chemicals. Methyl acrylate (3 moles; AR grade, Aldrich Chemical Co. Ltd), the alcohol (1.5 moles), *p*-toluene sulphonic acid (0.02 mole) and hydroquinone (0.005 mole) were added to a two-neck round-bottomed flask fitted with a fractional distillation assembly. The reaction mixture was refluxed steadily for one hour. The distillate was then collected under simultaneous distillation and rectification at a rate of about 10 $cm^3 h^{-1}$. The distillation temperature increased steadily from 63°C to 79°C throughout a period of 15–16 h, as first methanol and then methanol/methyl acrylate mixtures richer in methyl acrylate distilled off. The reaction mixture was then distilled under vacuum using the same assembly. The excess methyl acrylate and alcohol were distilled off. Then the required monomer was distilled. The first and last fraction of monomer were discarded. The middle fraction was collected and was used in the preparation of the polymer and the oligomer. n-Propyl acrylate distilled at 49.5°C and 92 mmHg; n-pentyl acrylate distilled at 51.5°C and 7 mmHg.

The n-butyl acrylate monomer was supplied by Aldrich Chemical Co. Ltd. It was purified by washing twice with aqueous sodium hydroxide solution (10% w/v), and then twice with distilled water. It was then dried with anhydrous sodium sulphate and fractionally distilled under reduced pressure. The fraction boiling at 35°C and 8 mmHg was collected.

The polymers were prepared by emulsion polymerization. The formulation used for the preparation was as follows:

Ingredients	*Parts by weight*
Double distilled water	100
Monomer	20
Potassium persulphate	0.01
Sodium lauryl sulphate	0.5
Dodecane-1-thiol	0.005

Potassium persulphate and sodium lauryl sulphate were obtained from BDH Chemicals (AR grade). Dodecane-1-thiol was obtained from Aldrich Chemical Co. Ltd. The potassium persulphate was further purified by recrystallization from distilled water. The other reagents were used as supplied. Water and the water-soluble ingredients were charged into a round-bottomed flask equipped with a stirrer, reflux condenser and thermometer. The flask was flushed with nitrogen and the monomer was added. The mixture was heated to 85°C under nitrogen atmosphere for 8 h and then at 90°C for 2 h. The hot emulsion was then poured slowly into three times its volume of hot (85°C) rapidly stirred sodium chloride (5% w/v) solution. The precipitated polymers were washed with a large amount of water, dried and purified by dissolving in butanone (BDH Chemicals, AR grade) and reprecipitating into distilled water. The purification procedure was carried out three times. Finally, the polymers were dried in a vacuum oven at 50°C until no further weight loss was observed.

Preparation of oligomers

The acrylate oligomers were prepared by a solution polymerization technique similar to that used by Shimomura[22]. A typical preparation uses inhibitor-free monomer (1 mole), isopropanol (30 moles; chain transfer agent, AR grade) and azobisisobutyronitrile (0.15 mole; initiator). The materials were introduced into a flask and nitrogen was bubbled through for 10 min to remove dissolved oxygen. The mixture was heated and stirred under reflux for 12 h. The solution was cooled, filtered and evaporated to dryness. The viscous oligomers were then dried in a vacuum oven at 50°C until no further weight loss was observed.

The oligomeric analogue of PVC was prepared by chlorination of a commercial oligomeric chlorinated paraffin (Cereclor S52, ICI), which had been previously used as an analogue for PVC[9]. Cereclor S52 was introduced into a three-necked round-bottomed flask fitted with a condenser, nitrogen inlet and chlorine inlet. It was gradually heated up to 70°C under a nitrogen atmosphere while being stirred by a magnetic stirrer. The flow rate of nitrogen was reduced and chlorine was passed through the Cereclor S52 at an average flow rate of 25 $cm^3 min^{-1}$. The chlorine gas was first passed through concentrated sulphuric acid and then over sodium hydroxide pellets. A tungsten lamp light source was used as a radical initiator. The chlorine flow continued for 12 h, after which the supply of chlorine was stopped and the flow rate of nitrogen was increased to remove any unreacted chlorine. The product was then dried in vacuum oven at 70°C until no further weight loss was observed. As the product contained approximately 57 wt% chlorine, it is henceforth referred to as oligomer S57. The S57 was found to have 57.2 wt% chlorine by elemental analysis (PVC is 56.8 wt%).

Preparation of blends

Blends were prepared by casting from a common solvent. The polymers in various proportions were dissolved to a total of 2% (w/v) in butanone (BDH Chemicals, AR grade, dried over molecular sieve). The solutions were poured into a Petri dish, and the solvent was allowed to evaporate to produce clear films. The film was kept under vacuum at 30°C until no further weight loss was observed.

Gel permeation chromatography

This was carried out using an Applied Chromatograph system with tetrahydrofuran as a solvent. Molecular weights were determined relative to polystyrene standards. The results are shown in *Table 1*.

Table 1 Molecular weights of polymers and oligomers

Polymer	$\bar{M}_n$	$\bar{M}_w$	$\bar{M}_w/\bar{M}_n$
PPrA	130 000	340 000	2.6
PBA	123 000	383 000	3.1
PPeA	180 000	415 000	2.3
PVC	74 000	170 000	2.3
Oligomer	$\bar{M}_n$	$\bar{M}_w$	$\bar{M}_w/\bar{M}_n$
PPrA	1180	3080	2.6
PBA	1450	3770	2.6
PPeA	1650	4125	2.5
S57	500[a]		

[a] Estimate based on known $\bar{M}_n$ for S52. Material too low for g.p.c.

Dynamic mechanical measurement

This was carried out using a 'dynamic mechanical thermal analyser' (model PL-DMTA, Polymer Laboratories Ltd). A strip of the sample was subjected to an imposed oscillatory frequency of 10 Hz. A temperature range of -70°C to 120°C was scanned at 4°C min^{-1} heating rate. A maximum in tan δ was taken as a measure of the glass transition temperature (T_g). A single peak suggests a homogeneous blend whereas two separate peaks suggest a two-phase structure.

Differential thermal analysis

Measurements were made with a Perkin–Elmer DSC II thermal analyser. Sample sizes of 50–60 mg were used, with a sensitivity of 8.4×10^{-4} J s^{-1}. The samples were cooled at -55°C and then scanned with a heating rate of 5°C min^{-1}.

Electron microscopy

The phase-separation process was observed by using electron microscopy. Samples were heated to a series of temperatures for up to 30 min, and then quenched with liquid nitrogen. Specimens about 900–1000 Å thick were cut with an ultramicrotome (LKB) equipped with a liquid-nitrogen-cooled cold chamber. A JEM 100B transmission electron microscope was used. The blend morphology was compared to the polymer blend without prior heat treatment.

Cloud-point determination by light-scattering turbidimetry

Phase boundaries were determined by measuring light scattered from the samples using a specially designed light-scattering turbidimeter[23]. The films of the polymer blends were supported in a sample holder located in a thermostically controlled aluminium block. Light from a tungsten lamp was focused onto the sample, and the light scattered at 45°C was measured by a photodiode. The temperature of the block could be altered at a controlled rate and a plot of scattered light against temperature was obtained. Results were corrected for changes in sensitivity of the diode with temperature. Abrupt increases in scattered light were considered as evidence of a cloud point. The samples could also be held at a preset temperature, and the increase in scattering observed as a function of time. The temperature at which a gradual increase in scattering occurred could be obtained, and this gives a much more reliable measure of the cloud point.

Heats of mixing

The heats of mixing were measured with a modified NBS batch-type calorimeter[23]. The calorimeter was calibrated with a heating coil immersed in the particular system under investigation. The calorimeter has an accuracy of ± 0.02 J g^{-1} as determined by an acid–base reaction. However, the viscosity of the oligomers makes mixing more difficult and we estimate an error of ± 0.1 J g^{-1} for our systems.

Measurement of specific volume

The specific volume of pure components was obtained by equal-density titration as described in ref. 24. Mixtures of saturated sodium bromide solution and distilled water were used. The densities of the sodium bromide solutions were measured by a liquid densitometer (DMA 46, Anton Paar, Austria). The instrument was calibrated with dry air at atmospheric pressure and with double distilled water at 25.0°C. Results are shown in *Table 2*.

Measurement of thermal expansion coefficient

The thermal expansion coefficients were determined by dilatometry as described by Orwoll and Flory[25]. A known amount of polymer was placed in the dilatometer container, which has a total volume of about 1 cm^3. The container was then filled with clean mercury. Air bubbles were removed under vacuum, and the volume expansions of the materials were measured in the range of 30–50°C. The results are shown in *Table 3*. The value for PVC was obtained from an extrapolation of results above the glass transition from the literature[26]. A value of T^* from the Simha–Somcynsky equation of state is presented, from which an estimate of the expansion coefficient can be made as $(3/2T^*)(T/T^*)^{1/2} \times 23.835$. The value of 5.34×10^{-4} seems reasonable compared to a value of 5.6×10^{-4} found by pressure dilatometry for a sample of PVC containing a small amount of plasticizer[27].

RESULTS AND DISCUSSION

The miscibility of polymers

From the glass-transition-temperature measurements, the blends of PVC with PPrA, PBA and PPeA show one single T_g, which indicates miscibility, and the results are shown in *Figures 1*, *2* and *3* respectively. For miscible polymer blends the T_g *versus* composition curve is not a universally similar relationship, but has many variations, similar to those observed with random copolymers. Using the Fox equation[28], the T_g values of the blends of PVC with PPrA, PBA and PPeA were calculated and are also shown in *Figures 1*, *2* and *3*.

The blends of PVC with PPrA and PBA show a positive deviation from the Fox equation, implying strong intermolecular interactions between the constituents of the blends. However, for the blends of PVC with PPeA, a negative deviation was observed. Since poly(n-hexyl acrylate) was found to be immiscible with PVC[3], it may suggest that PPeA exhibits a transitional behaviour from immiscibility to miscibility

Table 2 Densities and specific volumes of pure components (temperature of measurement, 25.0°C)

Material	Density, ρ (g cm^{-3})	Specific volume, v_{sp} (cm^3 g^{-1})
PPrA	1.0555	0.9474
PBA	1.0363	0.9650
PPeA	1.0167	0.9836
S57	1.3250	0.7547
Oligo-PPrA	1.0429	0.9589
Oligo-PBA	1.0225	0.9780
Oligo-PPeA	1.0116	0.9855
PVC	1.3920	0.7184

Table 3 State parameters of pure components

Component	$\alpha \times 10^4$ (K^{-1})	γ (J cm^{-3} K^{-1})	v_{sp} (cm^3 g^{-1})	S_2/S_1
PVC	5.34	1.20	0.718	–
PPrA	6.88	1.07	0.947	1.06
PBA	6.93	1.04	0.965	1.05
PPeA	7.01	1.02	0.965	1.05

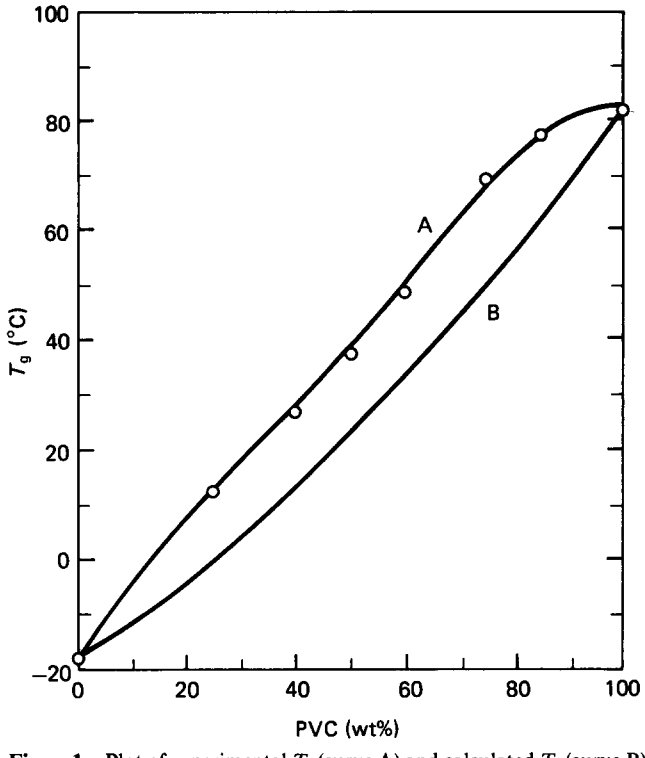

Figure 1 Plot of experimental T_g (curve A) and calculated T_g (curve B) using the Fox equation for blends of PVC/PPrA

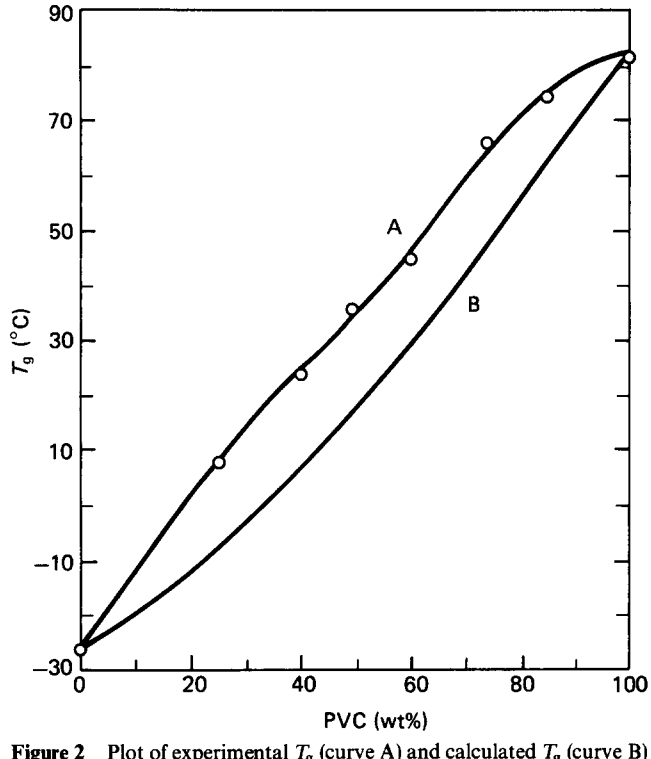

Figure 2 Plot of experimental T_g (curve A) and calculated T_g (curve B) using the Fox equation for blends of PVC/PBA

within the homologous series of acrylates with PVC, and hence it shows a negative deviation.

The phase separation was followed by differential thermal analysis. Samples of the film were heated for 1 h at a series of temperatures. The samples were then quenched and scanned as before. Phase separation was indicated when the single transition began to split into two component transitions. An example of this is shown in *Figure 4*. The phase-separation temperature can be identified within a fairly narrow range and the results by this method, when measured, agreed closely with those obtained by turbidimetry described below. The T_g values in principle contain information about the composition of the coexisting phases.

An experiment observing the phase separation of heat-treated samples by electron microscopy gave similar results. The phase-separated structures observed are shown in *Figures 5* and *6*. Phase separation is not

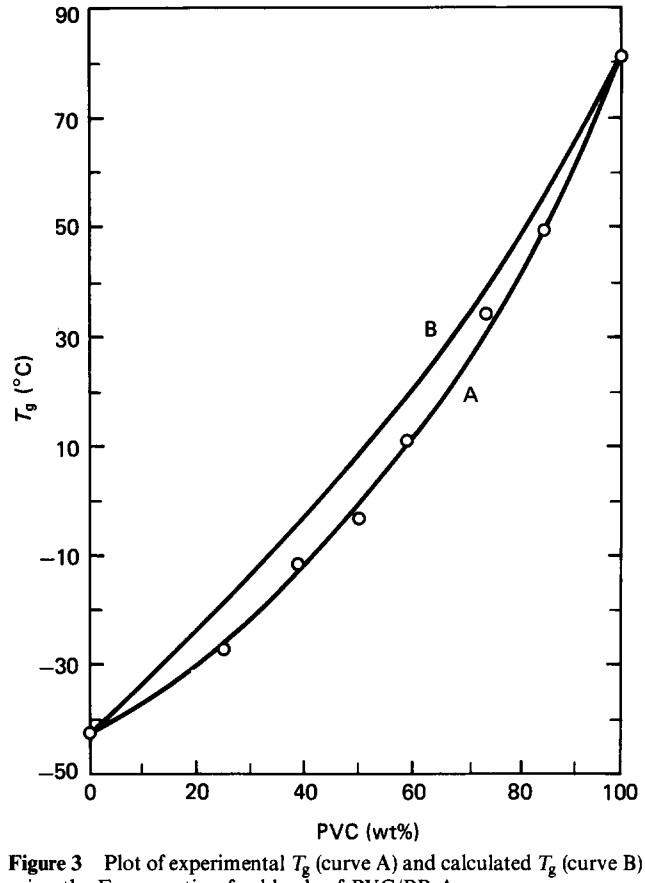

Figure 3 Plot of experimental T_g (curve A) and calculated T_g (curve B) using the Fox equation for blends of PVC/PPeA

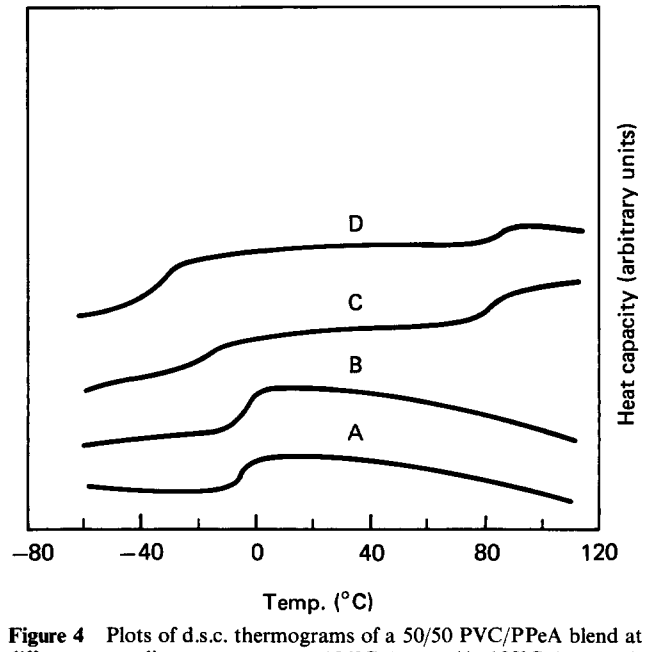

Figure 4 Plots of d.s.c. thermograms of a 50/50 PVC/PPeA blend at different annealing temperatures: 104°C (curve A), 105°C (curve B), 106°C (curve C) and 110°C (curve D)

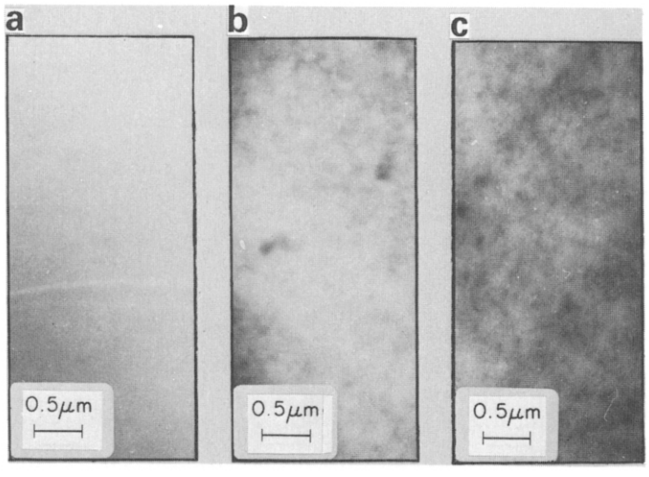

Figure 5 Transmission electron micrographs of a 50/50 PVC/PPrA blend: (a) not heat-treated; (b) annealed at 129°C for 10 min; (c) annealed at 129°C for 15 min

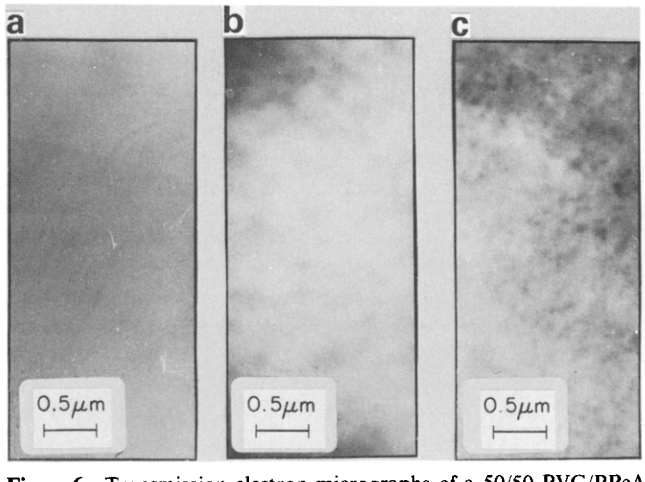

Figure 6 Transmission electron micrographs of a 50/50 PVC/PPeA blend: (a) not heat-treated; (b) annealed at 106°C for 10 min; (c) annealed at 106°C for 15 min

observed in unannealed samples but is seen on annealing. The phase structure becomes more clearly observable at greater times but it is difficult to make any conclusions concerning the growth of the phases.

The cloud-point curves for all the blends of PVC with PPrA, PBA and PPeA were determined by use of light-scattering turbidimetry. An example of the plots of scattering against temperature during a programmed heating run and during an isothermal scanning against time are shown in *Figure 7*. The phase diagrams for the three miscible blends studied by this method are shown in *Figure 8*. All three systems exhibit lower critical solution temperature (*LCST*) behaviour with phase-separation temperatures in the order of PPrA, PBA, PPeA. This trend is also found in the heats of mixing of the oligomeric analogues of polyacrylates and PVC, as shown in *Figure 9*.

One would expect that the higher concentration of interacting groups in PPrA would provide a higher degree of miscibility, but this is not found to the extent that might be expected, as a higher concentration of groups should lead to a significantly larger heat of mixing. The heats of mixing may also be affected by the contribution of the dispersive forces[8], which effectively produces a net counterbalance to the specific interaction contribution. The resultant heat of mixing would not be so negative and hence a lower *LCST* would be found.

Interactional energy calculation from heat-of-mixing data

In order to obtain the interactional energy X_{12} of the mixtures, the theoretical heat of mixing given by Flory's equation-of-state theory was fitted to the experimental heat of mixing. To utilize the heat-of-mixing equation, given as

$$\Delta H_m = \bar{r}NV^* \frac{\phi_1 P_1^*}{\tilde{v}_1} + \frac{\phi_2 P_2^*}{\tilde{v}_2} - \frac{P^*}{\tilde{v}} \qquad (22)$$

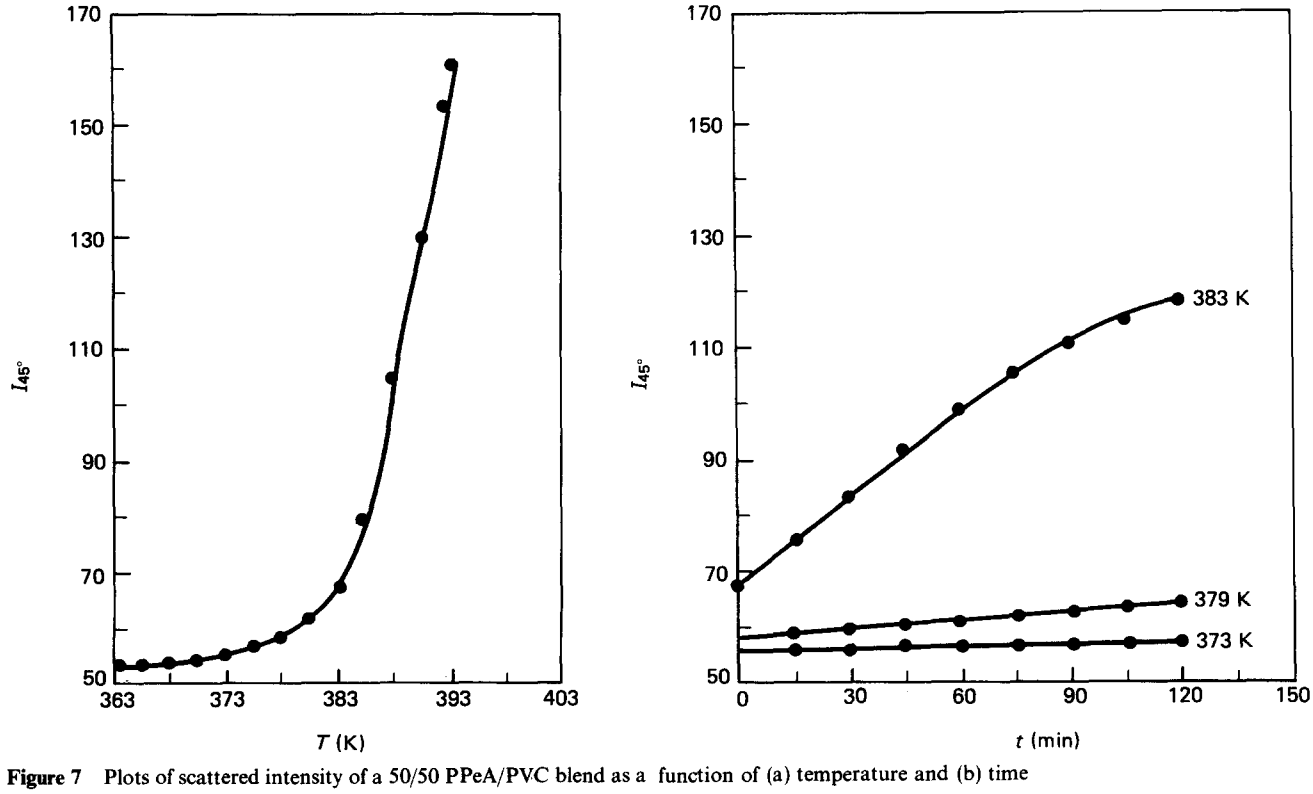

Figure 7 Plots of scattered intensity of a 50/50 PPeA/PVC blend as a function of (a) temperature and (b) time

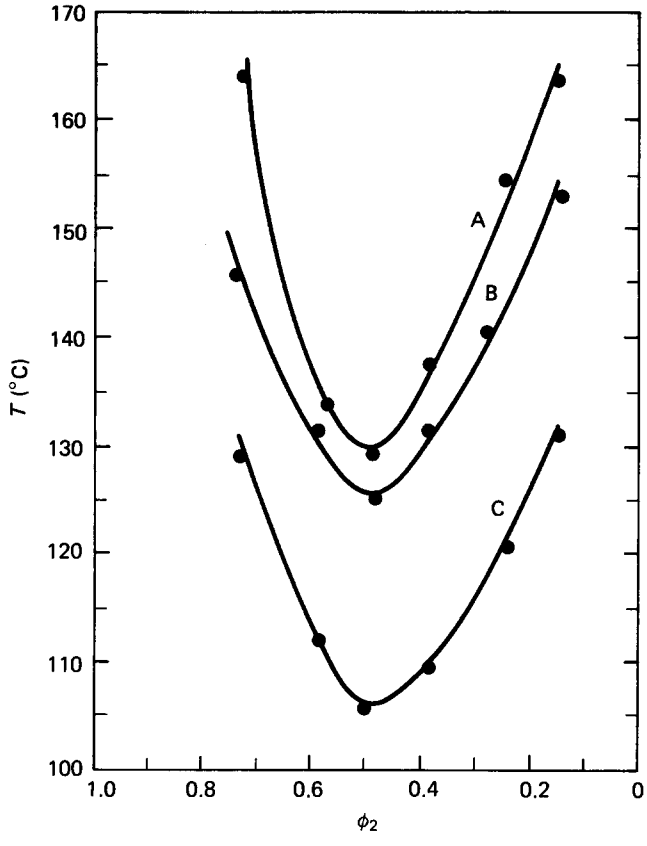

Figure 8 Phase diagrams of blends of PPrA (curve A), PBA (curve B) and PPeA (curve C) with PVC obtained by cloud-point measurements, plotted against volume fraction of the polyacrylates

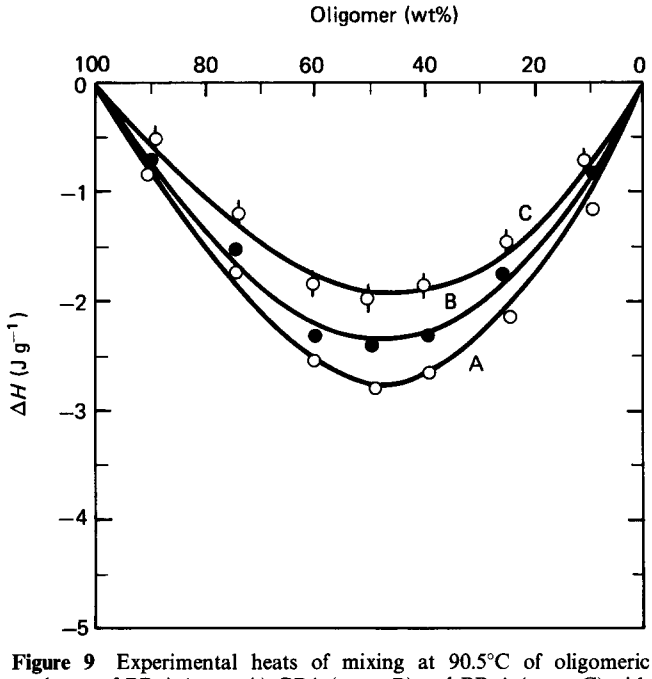

Figure 9 Experimental heats of mixing at 90.5°C of oligomeric analogue of PPrA (curve A), PBA (curve B) and PPeA (curve C) with S57, plotted against the weight per cent of the oligomeric analogues

the densities ρ, the thermal pressure coefficients γ and the thermal expansion coefficients α of the pure components are required. The density values of components were obtained by equal-density titration at 25°C. These were then approximately corrected to 70.0, 78.5 and 90.5°C, using expansion coefficients measured by dilatometry. This correction has only a very small effect on the calculated X_{12} values. Thermal pressure coefficients of the pure components were estimated from their solubility parameters and they, in turn, were calculated from the group contribution theory. This is not a very accurate procedure and the γ values are probably only reliable within 10%, but they do not have a very large effect on subsequent calculations. Details of this calculation are given elsewhere[18]. The binary parameter S_2/S_1 was estimated using Bondi's[29] group contribution data in the same manner as described elsewhere[18]. The thermal expansion coefficients of the pure polymers measured by dilatometry were used in the interaction-energy calculation. The expansion coefficient of the chlorinated polyolefin used was 6.5×10^{-4}, as reported for similar compounds[17]. Data used for the calculation are summarized in *Table 3*. The temperature dependence of these values was found by using equations (11), (12) and (13) respectively, and the values of $\tilde{v}$, P^* and $\tilde{T}$ were calculated using equations (14), (15) and (16). Knowing these quantities and a guessed value of X_{12}, one can calculate P^* of the mixture using equation (17). These values can be substituted in equation (4) in order to calculate values of ΔH_m. The value of X_{12} was varied until a best fit to the experimental ΔH_m values was obtained. An example of this fitting process is shown in *Figure 10* for the system of PVC and PBA at various temperatures. The values of X_{12} are tabulated in *Table 4*.

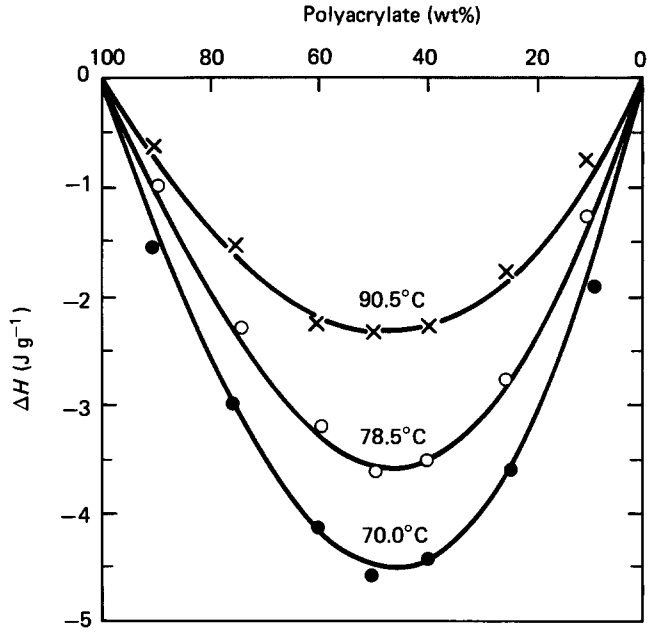

Figure 10 The heats of mixing for the PBA/PVC low-molecular-weight analogues at 90.5, 78.5 and 70.0°C plotted against the weight per cent of polyacrylate. The points show the experimental results and the curves were calculated for values of $X_{12} = -12.82$, -19.23 and -24.98 J cm^{-3} at 90.5, 78.5 and 70.0°C respectively

Table 4 Values of X_{12} and Q_{12} used for spinodal simulation

System	X_{12} (J cm^{-3})	Q_{12} (J cm^{-3} K^{-1})
PVC/PPrA	-15.11^a	$-3 \times 10^{-2\,a}$
	-0.14	-2.22×10^{-4}
PVC/PBA	-12.82^a	$-2.56 \times 10^{-2\,a}$
	-0.17	-2.36×10^{-4}
PVC/PPeA	-10.47^a	$-2.2 \times 10^{-2\,a}$
	-0.2	-2.25×10^{-4}

[a] Values obtained by fitting equation (4) to the experimental heats of mixing at 90.5°C, as described above

The value of X_{12} obtained in this way for oligomeric mixtures was assumed to be equivalent to that of the corresponding polymeric mixtures and was used for further calculations, as will be discussed later. This may not always give reliable results due to the differences between the high polymers and the analogues used, differences that arise from chain end effects, steric differences (in this case possibly due to differences in Cl distribution along the backbone) or density differences. A temperature dependence of X_{12} is observed for all of the systems studied. The gradual reduction of X_{12} for PVC/PPeA becomes more pronounced as the temperature increases towards the *LCST*. Similar behaviour can be observed for PVC/PBA and PVC/PPrA, but the effect on PVC/PPrA is not so marked as the others. This effect has been observed for chlorinated polyethylene with ethylene–vinyl acetate copolymers by Coleman *et al.*[21] when they studied the shift of the infra-red carbonyl absorption frequency against temperature. The relative shift does not become significant until the temperature approaches the respective phase-separation temperature. We would not therefore expect a marked decrease of X_{12} over the temperature range studied for PVC/PPrA, since all measurements are carried out at least 30° below the *LCST*.

Simulation of the spinodal curve

Using the value of X_{12} obtained from the heat of mixing of analogue oligomers at 90.5°C, together with the data given in *Table 3*, we have simulated the spinodal curves of PVC/PPrA, PVC/PBA and PVC/PPeA by means of equation (6). In these simulations a value of Q_{12} was chosen to match the minimum point of the spinodal curve to that of the cloud-point curve. The constant values of Q_{12} used are tabulated also in *Table 4*. The theoretical curves calculated are plotted together with the

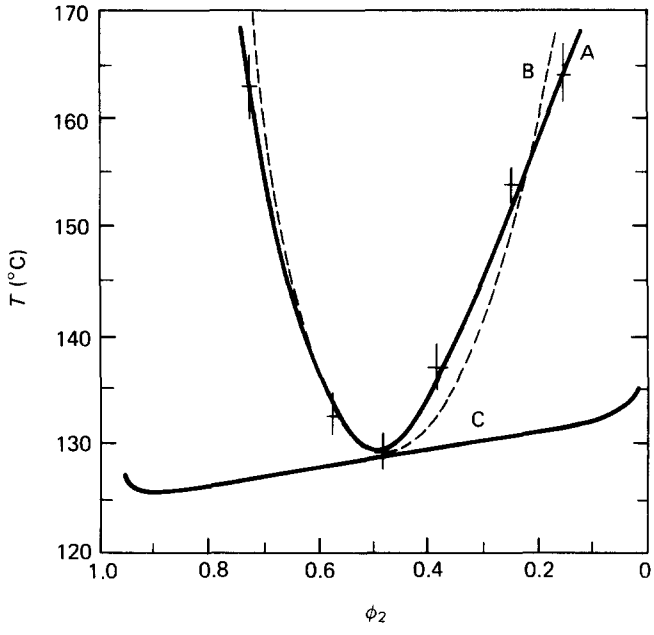

Figure 11 Simulated spinodal curves of PPrA/PVC blend using Flory's equation-of-state theory: curve A, experimental cloud-point curve; curve B, calculated using $X_{12} = -0.14\,J\,cm^{-3}$ and an adjusted value of $Q_{12} = -2.22 \times 10^{-4}\,J\,cm^{-3}\,K^{-1}$; curve C, calculated using $X_{12} = -15.11\,J\,cm^{-3}$ (obtained from heats of mixing of oligomeric analogues at 90.5°C) and an adjusted value of $Q_{12} = -3 \times 10^{-2}\,J\,cm^{-3}\,K^{-1}$

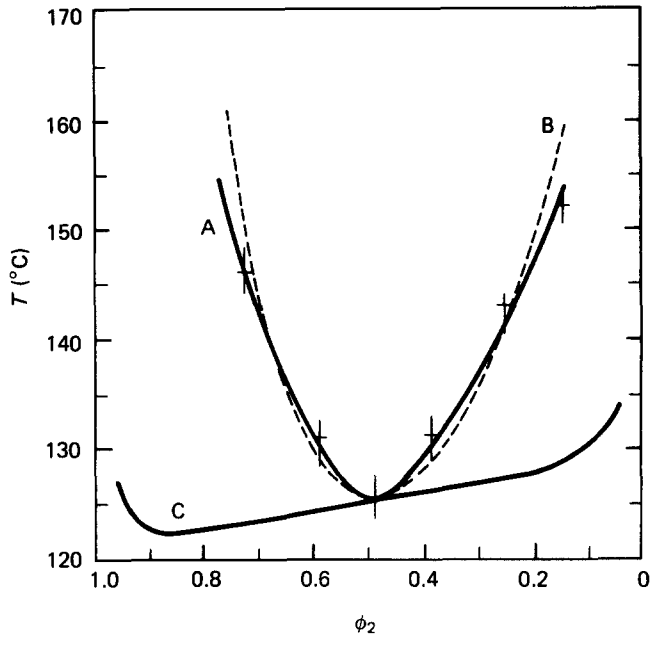

Figure 12 Simulated spinodal curves of PBA/PVC blend using Flory's equation-of-state theory: curve A, experimental cloud-point curve; curve B, calculated using $X_{12} = -0.17\,J\,cm^{-3}$ and an adjusted value of $Q_{12} = -2.36 \times 10^{-4}\,J\,cm^{-3}\,K^{-1}$; curve C, calculated using $X_{12} = -12.82\,J\,cm^{-3}$ (obtained from heats of mixing of oligomeric analogues at 90.5°C) and an adjusted value of $Q_{12} = -2.56 \times 10^{-2}\,J\,cm^{-3}\,K^{-1}$

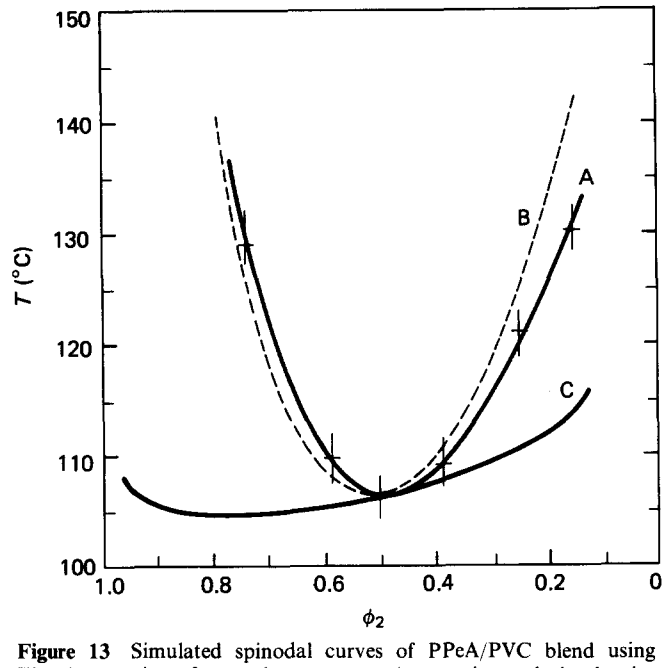

Figure 13 Simulated spinodal curves of PPeA/PVC blend using Flory's equation-of-state theory: curve A, experimental cloud-point curve; curve B, calculated using $X_{12} = -0.2\,J\,cm^{-3}$ and an adjusted value of $Q_{12} = -2.35 \times 10^{-4}\,J\,cm^{-3}\,K^{-1}$; curve C, calculated using $X_{12} = -10.47\,J\,cm^{-3}$ (obtained from heats of mixing of oligomeric analogues at 90.5°C) and an adjusted value of $Q_{12} = -2.2 \times 10^{-2}\,J\,cm^{-3}\,K^{-1}$

experimental phase boundaries for comparison in *Figures 11*, *12* and *13* respectively. It can be seen that the simulated spinodals are flat-bottomed and fall outside the miscibility gap, which is a thermodynamically unacceptable situation. In order to obtain a closer fit of simulated spinodals to the cloud-point curves, small negative X_{12} values were used accompanied with an adjustment of Q_{12} for fitting the minimum as mentioned above. The values were chosen to give a best fit of the

cloud points to the spinodal. One should note that the cloud point does not necessarily in practice coincide with the spinodal but should lie somewhere between the spinodal and binodal. The adjusted X_{12} and Q_{12} values used are shown in *Table 4*, and the calculated spinodals are also shown in *Figures 11*, *12* and *13*.

During the repetition of the simulation procedure, we found that a decrease in X_{12} would increase the curvature of the simulated spinodals. Furthermore, a lower Q_{12} value must be used for fitting the minima. A detailed study of the change in phase boundary by changing the other parameters (α, γ, X_{12} and molecular weight) using the same procedure was carried out on the system. The general trend observed is that:

(1) The higher the molecular weight of the system, the less miscible is the system.

(2) The thermal pressure coefficients of the binary components do not have a large effect in terms of the miscibility of two polymers. However, the critical point would tends towards compositions with higher volume fractions of the component having the higher γ value.

(3) The greater is the difference between the coefficient of thermal expansion of two polymers, the less miscible the system will become. However, for an increase of 5% in both components, the calculated spinodal would still fit the cloud-point curve with a small adjustment of the Q_{12} value, without changing the curvature.

(4) A large positive X_{12} value will bring about the immiscibility of the blends, and a large and negative X_{12} would ensure miscibility. A small negative X_{12} value would give a definite curvature to the simulated spinodal.

(5) A change in the value of S_2/S_1 by $\pm 10\%$ does not have much effect on the calculated spinodals.

Considering the assumptions made in the estimated state parameters, the simulated spinodals appear to have a good fit with the experimental cloud-point curve. Accounting for the errors in molecular weights and thermal expansion coefficients, the spinodal could still be simulated without change in curvature, although a different Q_{12} value has to be used.

It is not possible to fit the calculated spinodal to the experimental results without using Q_{12}. This is because the theory assumed that only interactions between neighbouring segments contribute to X_{12} and treated X_{12} as an enthalpy parameter, while the interactions between neighbours also affect the entropy. Furthermore, for a large favourable X_{12} (strong specific interaction), a large unfavourable Q_{12} is necessary and vice versa. Q_{12} could be interpreted as the unfavourable entropy change associated with the formation of the specific interaction. Therefore, it is apparent that the parameter Q_{12} plays an important role in the simulation of spinodal curves. On the whole, using X_{12} and Q_{12} as binary adjustable parameters, Flory's equation-of-state theory could be used to interpret qualitatively the polymer–polymer miscibility of homopolymer–homopolymer systems. However, one problem exists in applying the equation-of-state theory to these mixtures in that X_{12} is introduced as a temperature-independent constant whereas in many cases the heat of mixing, and hence X_{12}, is strongly temperature-dependent. This problem arises since X_{12} was never intended to describe the interactions between two polymers, which are dominated by a temperature-dependent specific interaction. The adjusted value of X_{12} may not, therefore, have any physical significance.

CONCLUSIONS

PVC was found to be miscible with PPrA, PBA and PPeA at all compositions at room temperature. They all show *LCST* behaviour and phase-separate at temperatures between 105 and 130°C. The polyacrylate with a higher concentration of carbonyl functional groups shows a higher *LCST* and hence is more miscible with PVC. This shows the significance of the specific interaction in causing miscibility and of the relative concentrations of interacting groups in determining the degree of compatibility and the temperatures of the phase-separation boundaries.

The phase boundaries of various systems can be described using the equation-of-state theory with a value of X_{12}, obtained from the heat of mixing of a low-molecular-weight analogue, and an empirical non-combinatorial entropy term, Q_{12}. The calculated spinodals are flat-bottomed. It was found that a much smaller negative X_{12} (and, hence, Q_{12}) can generate a spinodal with more curvature, which could better describe the experimental phase boundaries.

REFERENCES

1 Coleman, M. M. and Zaryan, J. *J. Polym. Sci., Polym. Phys. Edn.* 1979, **17**, 837; Coleman, M. M. and Varnall, D. F. *J. Polym. Sci., Polym. Phys. Edn.* 1980, **18**, 1403
2 Olabisi, O. *Macromolecules* 1975, **9**, 316
3 Walsh, D. J. and McKeown, J. G. *Polymer* 1980, **21**, 1330
4 Walsh, D. J. and McKeown, J. G. *Polymer* 1980, **21**, 1335
5 Walsh, D. J. and Cheong, G. L. *Polymer* 1982, **23**, 1965
6 Walsh, D. J. and Cheong, G. L. *Polymer* 1984, **25**, 495
7 Walsh, D. J. and Sham, C. K. *Polymer* 1984, **25**, 1023
8 Walsh, D. J. and Cheong, G. L. *Polymer* 1984, **25**, 499
9 McMaster, L. P. *Macromolecules* 1973, **6**, 760
10 Flory, P. J., Orwoll, R. A. and Vrij, R. *J. Am. Chem. Soc.* 1964, **86**, 3507, 3515
11 Flory, P. J. *J. Am. Chem. Soc.* 1956, **87**, 1833
12 Eichinger, B. E. and Flory, P. J. *Trans. Faraday Soc.* 1956, **64**, 2035
13 Flory, P. J., Ellenson, J. L. and Eichinger, B. E. *Macromolecules* 1967, **1**, 279
14 Olabisi, O. *Macromolecules* 1975, **8**, 316
15 Ten Brinke, G., Eshcies, A., Roerdenk, E. and Challa, G. *Macromolecules* 1981, **14**, 867
16 Chai, Z., Rouna, S., Walsh, D. J. and Higgins, J. S. *Polymer* 1983, **24**, 263
17 Chai, Z. and Walsh, D. J. *Makromol. Chem.* 1983, **184**, 1459
18 Rostami, S. and Walsh, D. J. *Macromolecules* 1984, **17**, 315
19 Walsh, D. J., Rostami, S. and Singh, V. B. *Makromol. Chem.* 1985, **186**, 145
20 Walsh, D. J. and Rostami, S. *Adv. Polym. Sci.* 1985, **70**, 119
21 Coleman, M. M., Maskala, E. J., Painter, P. C., Walsh, D. J. and Rostami, S. *Polymer* 1983, **24**, 1410
22 Shimomura, T. *Ind. Chem. Japan* 1968, **71**, 124
23 Cheong, G. L., Ph.D. Thesis, Imperial College, 1981
24 ASTM D1505-68, 1971
25 Orwoll, R. A. and Flory, P. J. *J. Am. Chem. Soc.* 1967, **89**, 6814
26 Simha, R., Wilson, P. S. and Olabisi, O. *Koll.-Z.Z. Polym.* 1973, **251**, 402
27 Zoller, P., private communication
28 Fox, T. G. *Bull. Am. Phys. Soc.* 1956, **1**, 123
29 Bondi, A. *J. Phys. Chem.* 1964, **68**, 441